First detection of c-C_3H_2 in a circumstellar disk

Chunhua Qi

Harvard-Smithsonian Center for Astrophysics, 60 Garden Street, Cambridge, MA 02138, USA

and

Karin I. Öberg

Departments of Chemistry and Astronomy, University of Virginia, Charlottesville, VA 22904, USA

and

David J. Wilner, Katherine A. Rosenfeld

Harvard-Smithsonian Center for Astrophysics, 60 Garden Street, Cambridge, MA 02138, USA

ABSTRACT

We report the first detection of c-C_3H_2 in a circumstellar disk. The c-C_3H_2 J=6 − 5 line (217.882 GHz) is detected and imaged through Atacama Large Millimeter Array (ALMA) Science Verification observations toward the disk around the Herbig Ae star HD 163296 at 0.8″ resolution. The emission is consistent with that arising from a Keplerian rotating disk. Two additional c-C_3H_2 transitions are also tentatively detected, bolstering the identification of this species, but with insufficient signal-to-noise ratio to constrain the spatial distribution. Using a previously developed model for the physical structure of this disk, we fit a radial power-law distribution model to the c-C_3H_2 6 − 5 emission and find that c-C_3H_2 is present in a ring structure from an inner radius of about 30 AU to an outer radius of about 165 AU. The column density is estimated to be 10^{12}–10^{13} cm^{-2}. The clear detection and intriguing ring structure suggest that c-C_3H_2 has the potential to become a useful probe of radiation penetration in disks.

Subject headings: protoplanetary disks; astrochemistry; stars: formation; ISM: molecules; techniques: high angular resolution; radio lines: ISM

1. Introduction

Pre-main sequence stars are commonly surrounded by disks, which serve the dual purpose of funneling accretion onto the central star and transporting away angular momentum. These disks are also the formation sites of planets and connect protostars and planets physically and chemically. The main component of gas-rich circumstellar disks, cold H_2, cannot be observed directly because of a lack of transitions at suitable energy levels. Instead, constraints on disk mass, density and temperature structures depend on observations of trace species, most commonly dust and CO gas (e.g. Qi et al. 2006; Piétu et al. 2007; Andrews et al. 2009). To access other disk properties, such as ionization levels, X-ray and UV radiation fields, turbulent mixing, chemical age and bulk composition requires the development of additional molecular probes whose formation and destruction depend critically on one or several of these properties.

The past decade has witnessed significant progress on disk chemistry theory, resulting in large numbers of predictions on how molecular abundance structures should depend on different disk properties (e.g. Aikawa & Nomura 2006; Willacy 2007; Semenov & Wiebe 2011; Fogel et al. 2011; Walsh et al. 2012). A lack of observational sensitivity has however limited detections to the simplest molecules in the millimeter/submillimeter range which characterizes the bulk of the gas disk, including CO, HCO^+, DCO^+, CN, HCN, DCN, C_2H, H_2CO, CS, SO, CH_2, N_2H^+ and HC_3N (Dutrey et al. 1997; Aikawa et al. 2003; Thi et al. 2004; Semenov et al. 2005; Dutrey et al. 2007; Qi et al. 2008; Fuente et al. 2010; Henning et al. 2010; Öberg et al. 2010, 2011). This list is expected to expand with the arrival of ALMA and its unprecedented sensitivity and spatial resolution, which will enable the development of a more diverse set of molecular probes. In this *Letter*, we use ALMA Science Verification observations of HD 163296 to report the first detection of cyclopropenylidene, c-C_3H_2, in a circumstellar disk. At a distance of ∼122 pc (Perryman et al. 1997), this Herbig Ae star (stellar mass 2.3 $M_\odot$; spectral type A1; age ∼4 Myr) harbors a large disk (a scattered light pattern extending out to a radius of ∼500 AU, Grady et al. 2000) with strong millimeter continuum and molecular line emission (Mannings & Sargent 1997; Thi et al. 2004; Natta et al. 2004; Isella et al. 2007; Qi et al. 2011). The large disk size and strong molecular emission make this system an ideal target to search for new molecules.

The c-C_3H_2 molecule is a small cyclic hydrocarbon, which was first detected in space by Thaddeus et al. (1985) towards Sgr B2. Since then, c-C_3H_2 has been detected in a wide range of astrophysical environments, including diffuse and dense clouds, protostars, planetary nebulae and extragalactic sources (e.g., Matthews & Irvine 1985; Cox et al. 1988, 1989; Madden et al. 1989; Benson et al. 1998; Menten et al. 1999; Fossé et al. 2001; Sakai et al. 2008; Tenenbaum et al. 2009; Liszt et al. 2012), and is one of the most abundant molecules

with 3 carbon atoms in the interstellar medium (Teyssier et al. 2004). In the context of disks, c-C_3H_2 has some favorable characteristics that may make it a powerful molecular probe, especially when observed in combination with isotopologues and chemically related molecules:

1. c-C_3H_2 has two equivalent H nuclei, which couple to generate ortho (nuclear spin of 1) and para (nuclear spin of 0) states. Deviations from the statistical weights of 3 to 1 may be used to constrain the formation conditions of the molecule (Park et al. 2006).

2. c-C_3H_2 is also one of two isomers; the other is the linear molecule l-C_3H_2. The isomer ratio can be used to assess the fractional ionization in clouds (Fossé et al. 2001) and may provide similar constraints on disks.

3. The formation and destruction chemistry of c-C_3H_2 (and carbon chains) are sensitive to high energy radiation. The vertical and radial abundance structure should provide strong constraints on the penetration depth of X-rays and UV photons (Semenov & Wiebe 2011).

4. Within the family of hydrocarbons, the sensitivity to turbulent mixing increases dramatically from C_2 to C_3H_2, and from C_3H_2 to larger hydrocarbons. Observed ratios and limits have the potential to constrain transport in disks (Semenov & Wiebe 2011).

Finally, the chemistry that produces c-C_3H_2 is important to constrain in its own right, since c-C_3H_2 shares precursors with other, more complex carbon chains, which may be an important source of carbon during planet formation. In light of these possibilities, we aim to provide first constraints on the abundance, distribution and o/p ratio of c-C_3H_2 in the HD 163296 disk.

2. Observations

HD 163296 (RA: $17^h56^m21^s.287$, DEC: $-21°57'22''.39$; J2000.0) was observed on 2012 June 9, June 23 and July 7 as part of the ALMA Science Verification (SV) program in band 6. At the time of observations, 25 12-m antennae were used (2 7-m ACA antennae were present in the dataset but flagged) in the array with a resulting synthesized beam size of $0.9\times0.7''$ (PA=84°). The source was observed with a total integration time of 84 minutes. The ALMA correlator was configured to simultaneously observe four spectral windows (two in each sideband). One of those windows (SpwID #1) covered both ^{13}CO and C^{18}O $2-1$ lines (220.399 and 219.560 GHz, respectively). The data were calibrated in the CASA software

package (v3.4), following the detailed calibration and imaging scripts provided by the ALMA science verification team. Since those scripts, along with fully calibrated measurement sets, are publicly available online[1], we do not repeat the details here. The 218 GHz (1.37mm) continuum was generated from the line-free channels in the two spectral windows (SpWID #0 and #1) of the lower sideband, and the flux is determined to be 608.5±2.5 mJy, which agrees with the SMA observations (Qi et al. 2011). Excellent agreement is also seen between the SMA and ALMA spectra for the ^{13}CO and C^{18}O $2-1$ lines with fluxes within 10% (Qi et al. 2011).

All of the c-C_3H_2 lines are continuum-subtracted and retrieved from SpwID #0 with a channel width of 0.488 MHz (0.67 km s^{-1}) covering the total 1.875 GHz bandwidth from 216.167 to 218.042 GHz. We have binned the lines in channels of 1 km s^{-1} to achieve higher signal-to-noise ratios and still keep the key kinematic features of the disk. The resulting line rms noise level is estimated to be 2.2 mJy beam^{-1} per 1 km s^{-1} channel in line free channels.

3. Results and Analysis

3.1. c-C_3H_2 detection

Figure 1 shows that the c-C_3H_2 $6-5$ line is clearly detected towards HD 163296 and that the position angle of its resolved velocity field is consistent with that of ^{13}CO from the same data set, which shows a clear pattern of Keplerian rotation. Interestingly, the c-C_3H_2 $6-5$ moment map displays a double-peaked morphology, indicative of an inner hole. The c-C_3H_2 $3-2$ and $5-4$ lines are only tentatively detected, insufficient to resolve the velocity field or any spatial structure. To improve the sensitivity in imaging these lines, we applied a Gaussian taper to the visibility data that corresponds to 1″ FWHM in the image domain, which resulted in a beam of 1.3×1.2″ (PA=78°).

Because the line emission changes position with channels, using a single mask for all channels to extract spectra will lead to a degradation of the signal. Instead, we create separate masks to cover the c-C_3H_2 $6-5$ line emission at each channel and use these masks to extract the line spectra. The same masks are also used for other c-C_3H_2 lines. Figure 2 shows the resulting spectra of all three c-C_3H_2 $3-2$ lines together with ^{13}CO $2-1$ line (with its own masks covering the ^{13}CO $2-1$ emission at each channel). The $6-5$ line is clearly detected with the expected line shape and V_{lsr} consistent with ^{13}CO. The $5-4$ line presents a consistent spectral profile, at lower signal-to-noise ratio. In contrast, the

[1]https://almascience.nrao.edu/almadata/sciver/HD163296Band6

$3-2$ line is both narrower and clearly blue-shifted, suggestive of a different physical origin, perhaps in a disk wind. However, both the $3-2$ and $5-4$ lines are observed at the edge of the spectral window, so this apparent asymmetry should be confirmed by independent observations before any strong conclusions are drawn.

The integrated fluxes are reported in Table 1. These are just below the upper limits reported in two previous failed searches of c-C_3H_2 in disks (Fuente et al. 2010; Öberg et al. 2010).

3.2. Ring structure model

We explore the distributions of c-C_3H_2 in HD 163296 based on a previously developed accretion disk model with well-defined temperature and density structures (Qi et al. 2011). To simulate and compare with the data, we assume the disk material orbits the central star in Keplerian motion, and fix the disk geometric and kinematic parameters that affect the observed spatio-kinematic behavior of the disk. The details of the stellar and accretion properties and the disk geometric and kinematic parameters are summarized in Table 3 of Qi et al. (2011). We have developed a physically self-consistent accretion disk model with an exponentially tapered edge that matches the spectral energy distribution and spatially resolved millimeter dust continuum emission. The disk temperature and density structures are further constrained by multiple CO and CO isotopologue line observations. Such analysis provides the essential framework for constraining the distribution of molecular abundances in protoplanetary disks.

Within this model framework, we assume that c-C_3H_2 is present with a constant abundance in a layer with boundaries toward the midplane and toward the surface of the disk (Qi et al. 2008; Öberg et al. 2012). This assumption is motivated by chemical models (e.g. Aikawa & Nomura 2006) that predict a three-layered structure where most molecules are photodissociated in the surface layer, frozen out in the midplane, and have an abundance that peaks at intermediate disk heights. The surface (σ_s) and midplane (σ_m) boundaries are presented in terms of $\Sigma_{21} = \Sigma_H/(1.59 \times 10^{21} cm^{-2})$, where Σ_H is the hydrogen column density measured from the disk surface in the adopted physical model. This simple model approach approximates the vertical location where c-C_3H_2 is most abundant. Due to the limited signal-to-noise of the multiple c-C_3H_2 line detections, we cannot constrain the location of this vertical layer based on the c-C_3H_2 data. We therefore fix the vertical surface boundary σ_s as 0.32 ($\log_{10}(\sigma_s) = -0.5$) and the midplane boundary σ_m as 3.2 ($\log_{10}(\sigma_m) = 0.5$), between which lies the expected location of most molecules with peak abundances in the warm molecular layer (Aikawa & Nomura 2006).

We model the radial column density distribution of c-C_3H_2 as a power law $N_{100} \times (r/100)^p$, where N_{100} is the column density at 100 AU in cm^{-2}, r is the distance from the star in AU, and p is the power-law index. Since the emission shows a clear indication of a central hole, we fit for both an inner radius R_{in} and outer radius R_{out} together with the power-law parameters (N_{100} and p). Using the structure model and the fixed vertical distributions, we compute a grid of synthetic c-C_3H_2 J=6 – 5 visibility datasets over a range of R_{out}, R_{in}, p and N_{100} values and compare with the observations. The best-fit model is obtained by minimizing χ^2, the weighted difference between the real and imaginary part of the complex visibility measured in the (u, v)-plane sampled by the ALMA observations. We use the two-dimensional Monte Carlo model RATRAN (Hogerheijde & van der Tak 2000) to calculate the radiative transfer and molecular excitation. The collisional rates are taken from Chandra & Kegel (2000) and the molecular data file is retrieved from the Leiden Atomic and Molecular Database (Schöier et al. 2005).

Figure 3 shows the χ^2 surfaces for the R_{in} and R_{out} versus the power law index p. We find the p is constrained between -2.5 and -1.5, R_{in} 15–40 AU and R_{out} 150–200 AU (within 1σ) with best-fit values at -2, 30 and 165 AU, respectively (reduced $\chi^2 = 1.07$). By fixing the above parameters at their best-fit values, N(c-C_3H_2) is determined to be 2.2±0.2 $\times 10^{12}$ cm^{-2} at 100 AU. Figure 4 presents comparisons between the observed channel maps and the best-fit model. The residual image doesn't show any significant emission, which indicates that the c-C_3H_2 emission is consistent with that arising from a Keplerian rotating disk. The $6-5$ line is actually blended with the $6_{1,6} - 5_{0,5}$ (ortho) and $6_{0,6} - 5_{1,5}$ (para) lines at the same frequency. Since the Einstein A-coefficients for both ortho and para lines are the same, 5.393×10^{-4} s^{-1} (Schöier et al. 2005), we fit the data with the ortho line only and the resulting column density can be accounted as the sum of both ortho and para forms of the molecule.

For the weaker $5-4$ ortho line, the signal-to-noise ratio is too low to provide any constraints on the c-C_3H_2 the distribution. By assuming the c-C_3H_2 distribution derived from the $6-5$ line, however, we can use the unresolved line flux to constrain the o/p ratio. The resulting best-fit N(C_3H_2-(o))=1.6±0.3 $\times 10^{12}$ and N(C_3H_2-($o+p$)=2.2±0.2 $\times 10^{12}$ cm^{-2} at 100 AU (as shown above). Hence o/p=2.7±1.7, which is close to the statistical value of 3, but the large uncertainty implies that better data are required to use this ratio as a probe of formation conditions.

4. Discussion

We have clearly detected c-C_3H_2 in the disk around HD 163296. This is one of the two largest molecules detected in disks so far, the other being HC_3N, also a carbon-chain molecule, detected recently using deep single-dish observations (Chapillon et al. 2012).

Using the spatially and spectrally resolved line emission, we have constrained the radial distribution of c-C_3H_2 in the HD 163296 disk as a ring structure ranging from ∼30 to ∼165 AU. The outer edge of <250 AU (2σ limit) is much smaller than the gas disk size which extends to 500 AU (Qi et al. 2011), which suggests that c-C_3H_2 formation is slow or that c-C_3H_2 destruction is fast in the outer disk. In terms of formation, the best-fit outer radius coincides with the previously determined location of the CO midplane snow line, and it is possible that CO freeze-out limits the carbon available in the gas phase to form hydrocarbons in general and c-C_3H_2 in particular. A second characteristic of the outer disk is that it is rather tenuous because of a rapidly decreasing column density outside of 200 AU (Qi et al. 2011). This may result in efficient penetration of radiation and thus destruction of the easily dissociated c-C_3H_2. Explicit model predictions are required to resolve which effect drives the disappearance of c-C_3H_2 in the outer disk.

No existing disk chemistry model in the literature contains predictions for the radial distribution of c-C_3H_2. Based on strong correlations found between c-C_3H_2 and CCH in several astrophysical environments (Lucas & Liszt 2000; Pety et al. 2005; Gerin et al. 2011), predictions on CCH in disks can be used to shed further light on the origins of c-C_3H_2. Aikawa & Herbst (2001) predicts a CCH central cavity in the absence of X-ray radiation; when X-rays are present, and HD 163296 is a known X-ray emitter (Swartz et al. 2005; Günther & Schmitt 2009), the CCH column is instead centrally peaked. Despite the presence of X-rays, the central cavity could be due to a UV dominated radiation field. This may be tested by observing c-C_3H_2 towards T Tauri stars with weak UV fields and strong X-rays, and towards additional Herbig Ae stars with weak X-rays.

The inner cavity could also be a product of the main formation pathway of c-C_3H_2. Carbon chains can form through at least three different pathways: (1) ion-neutral reactions at low temperatures, (2) photo-erosion of larger carbonaceous compounds, and (3) neutral-neutral reactions at luke-warm temperatures following CH_4 ice evaporation at ∼30 K (Herbst et al. 1984; Teyssier et al. 2004; Sakai et al. 2008; Gerin et al. 2011). Detailed modeling of c-C_3H_2 radial distributions in each of these formation scenarios are clearly needed to use c-C_3H_2 rings as tracers of the radiation field and other disk characteristics.

In addition to more detailed modeling, additional observations are needed to constrain whether different hydrocarbons, especially CCH and c-C_3H_2, are correlated in disk envi-

ronments, and to constrain the vertical distribution of these molecules. The latter requires multiple lines with a range of excitation energies. With the combined advance in theory and observations, c-C_3H_2 may become one of the more useful probes of penetration of the radiation fields in disks.

Facility: ALMA

This paper makes use of the following ALMA data: ADS/JAO.ALMA#2011.0.00010.SV. ALMA is a partnership of ESO (representing its member states), NSF (USA) and NINS (Japan), together with NRC (Canada) and NSC and ASIAA (Taiwan), in cooperation with the Republic of Chile. The Joint ALMA Observatory is operated by ESO, AUI/NRAO and NAOJ.
We would like to thank an anonymous referee for thoughtful suggestions for the paper. We also acknowledge NASA Origins of Solar Systems grant No. NNX11AK63.

REFERENCES

Aikawa, Y. & Herbst, E. 2001, A&A, 371, 1107

Aikawa, Y., Momose, M., Thi, W., et al. 2003, PASJ, 55, 11

Aikawa, Y. & Nomura, H. 2006, ApJ, 642, 1152

Andrews, S. M., Wilner, D. J., Hughes, A. M., Qi, C., & Dullemond, C. P. 2009, ApJ, 700, 1502

Benson, P. J., Caselli, P., & Myers, P. C. 1998, ApJ, 506, 743

Chandra, S., & Kegel, W. H. 2000, A&AS, 142, 113

Chapillon, E., Dutrey, A., Guilloteau, S., et al. 2012, ApJ, 756, 58

Cox, P., Guesten, R., & Henkel, C. 1988, A&A, 206, 108

Cox, P., Walmsley, C. M., & Guesten, R. 1989, A&A, 209, 382

Dutrey, A., Guilloteau, S., & Guelin, M. 1997, A&A, 317, L55

Dutrey, A., Henning, T., Guilloteau, S., et al. 2007, A&A, 464, 615

Fogel, J. K. J., Bethell, T. J., Bergin, E. A., Calvet, N., & Semenov, D. 2011, ApJ, 726, 29

Fossé, D., Cernicharo, J., Gerin, M., & Cox, P. 2001, ApJ, 552, 168

Fuente, A., Cernicharo, J., Agúndez, M., et al. 2010, A&A, 524, A19

Gerin, M., Kaźmierczak, M., Jastrzebska, M., et al. 2011, A&A, 525, A116

Grady, C. A., et al. 2000, ApJ, 544, 895

Günther, H. M., & Schmitt, J. H. M. M. 2009, A&A, 494, 1041

Henning, T., Semenov, D., Guilloteau, S., et al. 2010, ApJ, 714, 1511

Herbst, E., Adams, N. G., & Smith, D. 1984, ApJ, 285, 618

Hogerheijde, M. R. & van der Tak, F. F. S. 2000, A&A, 362, 697

Isella, A., Testi, L., Natta, A., Neri, R., Wilner, D., & Qi, C. 2007, A&A, 469, 213

Liszt, H., Sonnentrucker, P., Cordiner, M., & Gerin, M. 2012, ApJ, 753, L28

Lucas, R. & Liszt, H. S. 2000, A&A, 358, 1069

Mannings, V., & Sargent, A. I. 1997, ApJ, 490, 792

Matthews, H. E. & Irvine, W. M. 1985, ApJ, 298, L61

Madden, S. C., Irvine, W. M., Swade, D. A., Matthews, H. E., & Friberg, P. 1989, AJ, 97, 1403

Menten, K. M., Carilli, C. L., & Reid, M. J. 1999, in Astronomical Society of the Pacific Conference Series, Vol. 156, Highly Redshifted Radio Lines, ed. C. L. Carilli, S. J. E. Radford, K. M. Menten, & G. I. Langston, 218

Natta, A., Testi, L., Neri, R., Shepherd, D. S., & Wilner, D. J. 2004, A&A, 416, 179

Öberg, K. I., Qi, C., Fogel, J. K. J., et al. 2010, ApJ, 720, 480

Öberg, K. I., Qi, C., Fogel, J. K. J., et al. 2011, ApJ, 734, 98

Öberg, K. I., Qi, C., Wilner, D. J., & Hogerheijde, M. R. 2012, ApJ, 749, 162

Perryman, M. A. C., et al. 1997, A&A, 323, L49

Park, I. H., Wakelam, V., & Herbst, E. 2006, A&A, 449, 631

Pety, J., Teyssier, D., Fossé, D., et al. 2005, A&A, 435, 885

Piétu, V., Dutrey, A., & Guilloteau, S. 2007, A&A, 467, 163

Qi, C., D'Alessio, P., Öberg, K. I., et al. 2011, ApJ, 740, 84

Qi, C., Wilner, D. J., Aikawa, Y., Blake, G. A., & Hogerheijde, M. R. 2008, ApJ, 681, 1396

Qi, C., Wilner, D. J., Calvet, N., et al. 2006, ApJ, 636, L157

Sakai, N., Sakai, T., & Yamamoto, S. 2008, Ap&SS, 313, 153

Schöier, F. L., van der Tak, F. F. S., van Dishoeck, E. F., & Black, J. H. 2005, A&A, 432, 369

Semenov, D., Pavlyuchenkov, Y., Schreyer, K., et al. 2005, ApJ, 621, 853

Semenov, D. & Wiebe, D. 2011, ApJS, 196, 25

Swartz, D. A., Drake, J. J., Elsner, R. F., et al. 2005, ApJ, 628, 811

Tenenbaum, E. D., Milam, S. N., Woolf, N. J., & Ziurys, L. M. 2009, ApJ, 704, L108

Teyssier, D., Fossé, D., Gerin, M., et al. 2004, A&A, 417, 135

Thaddeus, P., Vrtilek, J. M., & Gottlieb, C. A. 1985, ApJ, 299, L63

Thi, W., van Zadelhoff, G., & van Dishoeck, E. F. 2004, A&A, 425, 955

Walsh, C., Nomura, H., Millar, T. J., & Aikawa, Y. 2012, ApJ, 747, 114

Willacy, K. 2007, ApJ, 660, 441

Table 1: c-C_3H_2 line results.

Transition	Frequency (GHz)	E_u (K)	Beam	$\int F dv$ (mJy km s^{-1})
$3_{3,0} - 2_{2,1}$	216.279	19	$1\farcs3 \times 1\farcs2(76°)$	53[9]
$6_{1,6} - 5_{0,5}/6_{0,6} - 5_{1,5}$	217.822	39	$0\farcs9 \times 0\farcs7(83°)$	185[10]
$5_{1,4} - 4_{2,3}$	217.940	35	$1\farcs3 \times 1\farcs2(78°)$	74[9]

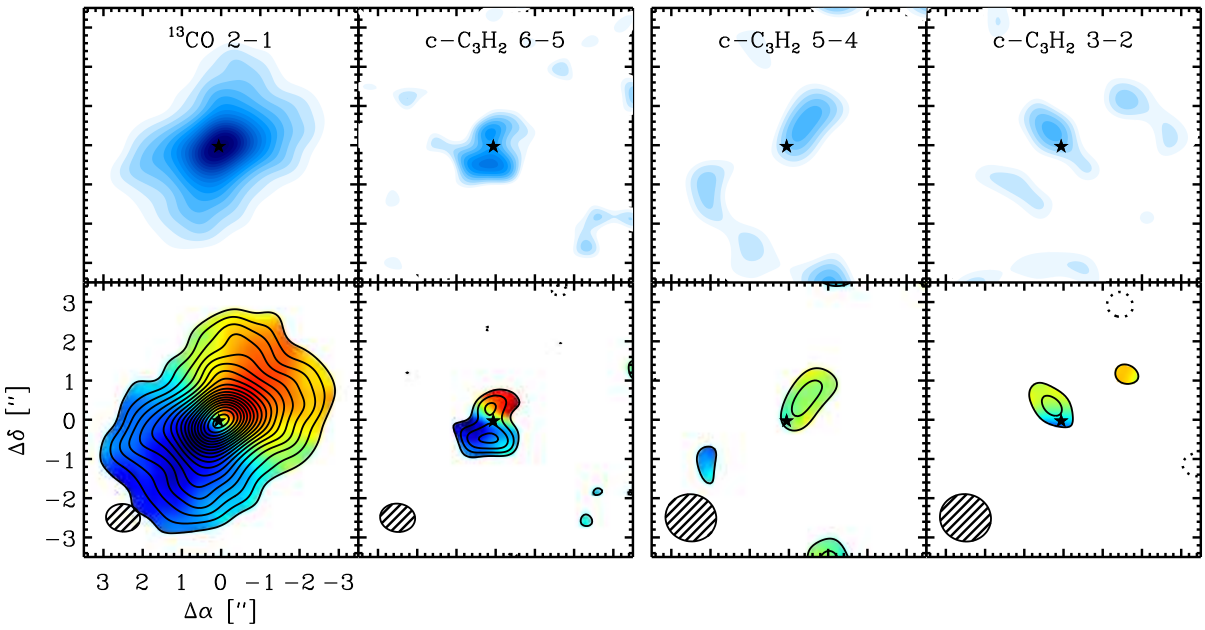

Fig. 1.— The integrated intensity maps summed between 0 and 11 km s^{-1}) and intensity-weighted mean velocity fields of ^{13}CO $2-1$ and c-C_3H_2 $6-5$ lines (left panel), c-C_3H_2 $5-4$ and $3-2$ lines (right panel) toward HD 163296. The resolved velocity field of the c-C_3H_2 $6-5$ line agrees with the CO kinematics. In the c-C_3H_2 maps, the first contour marks 3σ followed by 1σ contour increases. The rms varies between 6 and 9 mJy km s^{-1} per beam. Synthesized beams are presented in the lower left corners. The star symbol indicates the continuum (stellar) position. The axes are offsets from the pointing center in arcseconds.

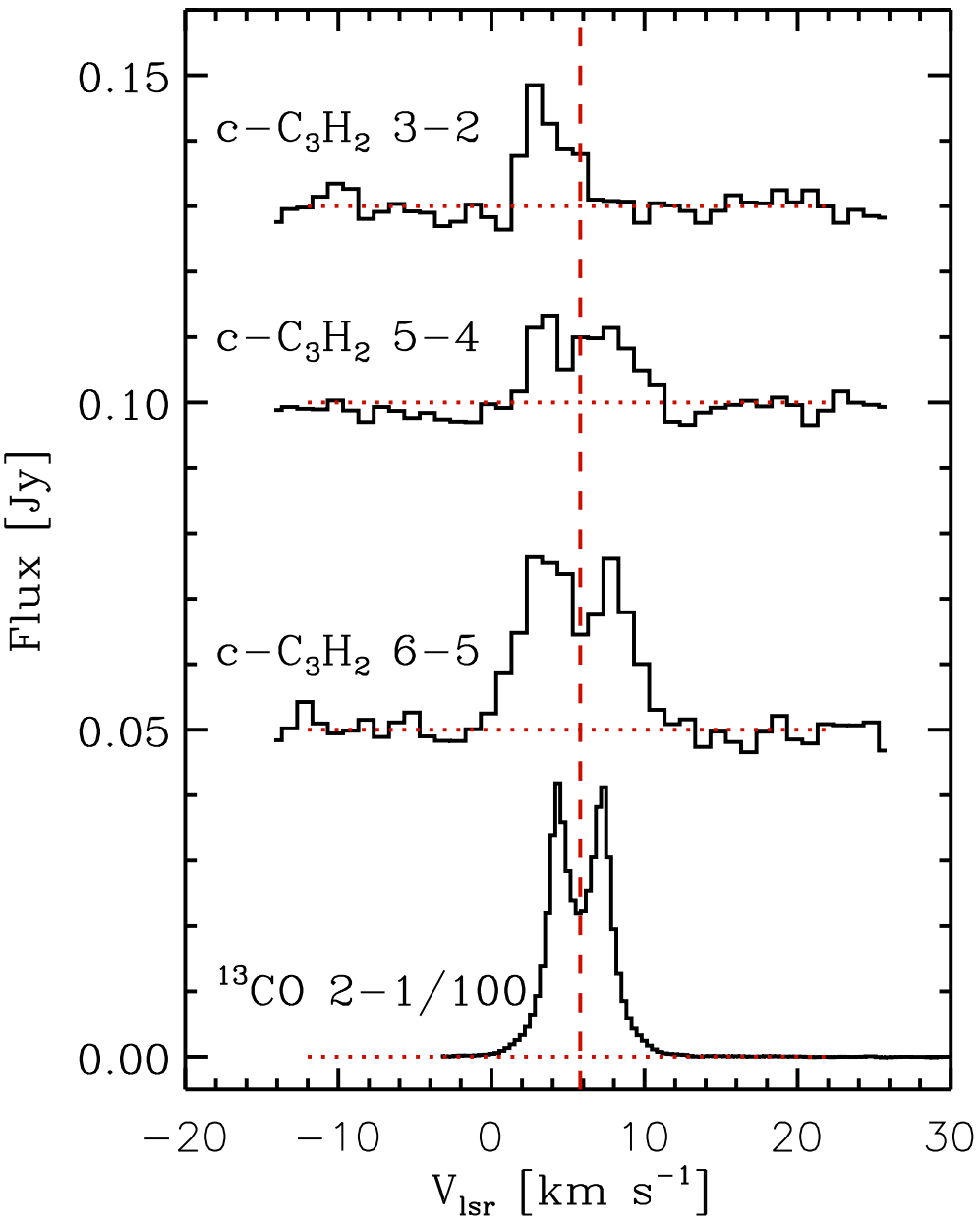

Fig. 2.— Extracted spectra of the three c-C_3H_2 transitions toward HD 163296, plotted together with ^{13}CO $2-1$. The dashed line marks V_{LSR} toward HD 163296.

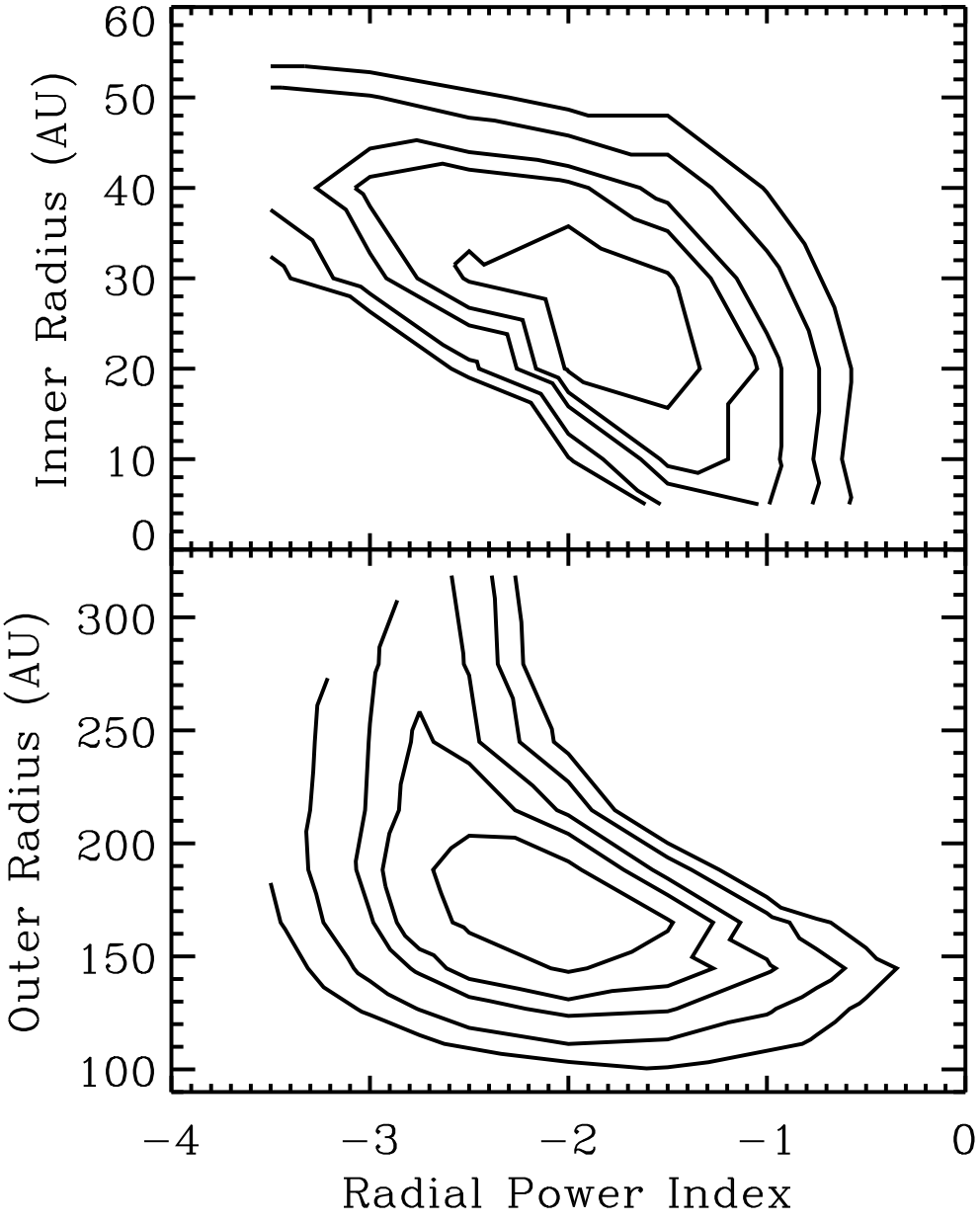

Fig. 3.— Iso-χ^2 surfaces of $R_{\rm out}$ and $R_{\rm in}$ versus p. Contours correspond to the 1–5 σ errors.

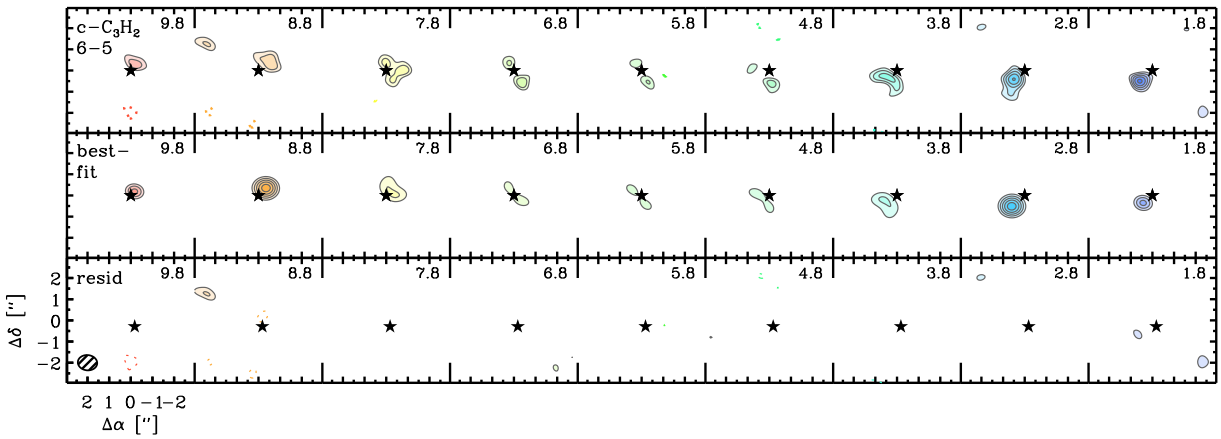

Fig. 4.— The top panel shows the velocity channel map of the c-C_3H_2 $6-5$ emission toward HD 163296 (velocities binned in 1 km s^{-1}). Contours are 0.0022 Jy Beam^{-1} (1σ) $\times[3, 4, 5, 6, 7, 8, 9]$. The middle and bottom panels show the best-fit model and the difference between the best-fit model and data on the same contour scale. The star symbol indicates the continuum (stellar) position. The axes are offsets from the pointing center in arcseconds.